Environmental Technology, Vol. 27. pp 219-232

DEGRADATION KINETICS AND MECHANISM OF RDX AND HMX IN TiO_2 PHOTOCATALYSIS

J-K. CHOI[1], H-S. SON[1], T-S. KIM[1], M. K. STENSTROM[2] AND K-D. ZOH[1]*

[1]Institute of Health & Environment, School of Public Health, Seoul National University, Seoul, 110-799, Korea
[2]Dept. of Civil & Environmental Engineering, University of California, Los Angeles, CA 90095, USA

(Received 4 March 2005; Accepted 16 October 2005)

ABSTRACT

This study was undertaken to examine the photocatalytic degradation of explosives hexahydro-1,3,5-trinitro-1,3,5-triazine (RDX) and octahydro-1,3,5,7-tetranitro-1,3,5,7-tetrazocine (HMX) with a circular photocatalytic reactor, using a UV lamp as a light source and TiO_2 as a photocatalyst. The effects of various parameters, such as the RDX or HMX concentration, the amount of TiO_2, and the initial pH, on the photocatalytic degradation rates of explosives were examined. In the presence of both UV light and TiO_2, RDX and HMX were more effectively degraded than with either UV or TiO_2 alone. The degradation rates were found to obey pseudo-first-order kinetics represented by the Langmuir-Hinshelwood model. Increases in the RDX and HMX degradation rates were obtained with decreasing initial concentrations of the explosives. The RDX and HMX degradation rates were higher at pH 7 than at either pH 3 or pH 11. A dose of approximately 0.7 g l^{-1} of TiO_2 degraded HMX more rapidly than did higher or lower TiO_2 doses. RDX (20 mg l^{-1}) photocatalysis resulted in an approximately 20% decrease in TOC, and HMX (5 mg l^{-1}) photocatalysis resulted in a 60% decrease in TOC within 150 minutes. A trace amount of formate was produced as an intermediate that was further mineralized by RDX or HMX photocatalysis. The nitrogen byproducts from the photocatalysis of RDX and HMX were mainly NO_3^- with NO_2^- and NH_4^+. The total nitrogen recovery was about 60% from RDX (20 mg l^{-1}), and 70% from HMX (5 mg l^{-1}), respectively. Finally, a mechanism for RDX/HMX photocatalysis was proposed, along with supporting qualitative and quantitative evidence.

Keywords: Hexahydro-1,3,5-trinitro-1,3,5-triazine (RDX), octahydro-1,3,5,7-tetranitro-1,3,5,7-tetrazocine (HMX), TiO_2, photocatalysis, mineralization

INTRODUCTION

Hexahydro-1,3,5-trinitro-1,3,5-triazine (RDX) and octahydro-1,3,5,7-tetranitro-1,3,5,7-tetrazocine (HMX), along with 2,4,6-trinitrotolune (TNT), are among the most common explosives in the world. HMX and RDX are often found in the soil, groundwater, and surface waters near facilities where they are manufactured, owing to negligent disposal methods such as dumping into unlined pits, disposal in lagoons, and open burning/open detonation (OB/OD) [1,2]. Figure 1 shows the chemical structure of RDX and HMX.

RDX is toxic to aquatic and terrestrial organisms [3-5], tends to persist in the environment [6], and is typically found together with HMX [7]. The US EPA has classified RDX as a possible human carcinogen (Class C) and has set the ambient criteria for RDX and HMX at 0.3 mg l^{-1}. Drinking water criteria require RDX levels of less than 0.035 mg l^{-1} [8, 9]. The health advisory for lifetime exposure to RDX and HMX has been set at 0.002 and 0.4 mg l^{-1}, respectively [7, 10].

Advanced oxidation processes (AOP) are commonly used for remediating wastewaters contaminated with recalcitrant organic pollutants. Among these processes, the photocatalytic degradation of recalcitrant organic contaminants in the presence of titanium dioxide (TiO_2) has recently been of interest [11, 12]. Photocatalysis is potentially important in the treatment of water and wastewaters because the process is relatively rapid, capable of simultaneously degrading a wide range of contaminants. The degradation of RDX using AOP processes such as UV/H_2O_2, ozone, ozone/H_2O_2, UV/ozone [13, 14] and Fenton oxidation [15] has been reported. However, the detailed kinetics and the mechanism of RDX and HMX in TiO_2 photocatalysis have not been extensively examined.

The possibility of degrading RDX and HMX using photocatalysis was reported earlier [16] using a TiO_2 slurry circular photoreactor. This paper extends the earlier work

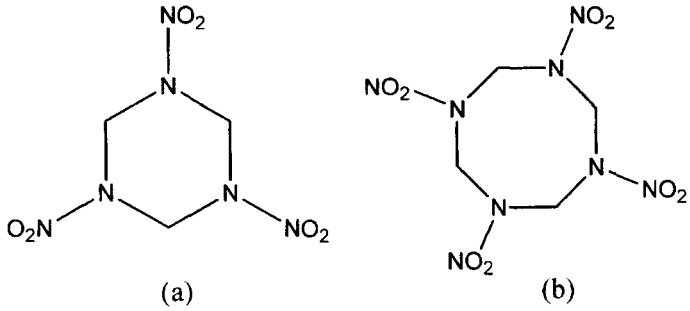

Figure 1. Structures of (a) RDX and (b) HMX

and examines the kinetics and mechanisms of photocatalytic degradation of RDX and HMX in the same system with the objective of determining end products and mechanisms. The effects of various parameters, such as the initial concentrations of the explosives, the TiO_2 dosage, and the initial pH of the solution, on the degradation efficiency of RDX and HMX were investigated to determine the optimum treatment conditions. The identification and quantification of principal degradation byproducts were examined using HPLC, ion chromatography, and TOC.

MATERIALDS AND METHODS

Chemicals

Pure RDX and HMX were obtained from the Korean Agency for Defense Development. The RDX and HMX were dried for 24 h in desiccators before being dissolved in deionized water. As RDX and HMX are moderately to weakly soluble in water at 60 mg l^{-1} and 5 mg l^{-1} at 25°C, respectively [17], aqueous stock solutions containing 40 mg l^{-1} RDX or 5 mg l^{-1} HMX were prepared by dissolving pure RDX and HMX at moderate heat with stirring for 24 h. The TiO_2 powder used as the photocatalyst was Degussa P-25 (Degussa Chemical Co., Germany).

Photoreactor System

The photocatalytic degradation experiments were performed in a circulating photoreactor system (Figure 2). The reactor system consisted of a reservoir, a metering pump (Cole-Parmer, Chicago, IL) for the circulation of the reactor contents, and a photoreaction chamber, all connected with flexible Teflon tubing. The reservoir consisted of a 1-l glass bottle, and the reaction solution was stirred to maintain uniformity. The RDX/HMX solution was circulated to the photoreaction chamber by a metering pump at a flow rate of 1-l min^{-1}. The UV chamber consisted of four UV lamps and five photoreactor columns. The reactor columns each consisted of a cylindrical quartz tube, with an outside diameter of 10 mm and a length of 100 cm. Since the internal diameter is approximately 0.80 cm, the volume of each tube is around 80.0 ml (0.80 cm x 100 cm). Therefore, the total volume of five quartz tubes is 400.0 ml.

The reactor assembly was illuminated by four UV lamps, each with a diameter of 30 mm and a length of 100 cm. In contrast with most photocatalysis researches that used strong UV lamp higher than 100 W in order to treat organic compounds or inactivate the microorganisms [18,19], the UV

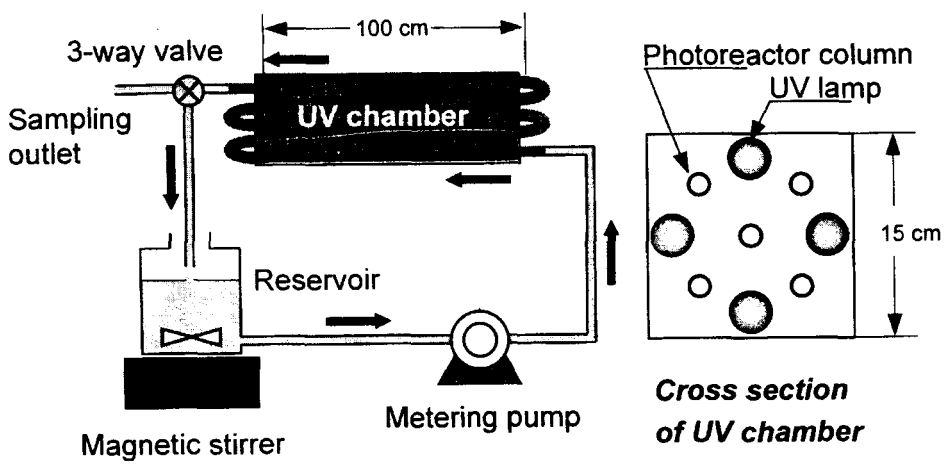

Figure 2. Schematic of the photocatalytic reactor.

lamps with a low energy power input of 15-W emitting approximately 90% of their radiation at 254 nm was used in this study. The UV lamps, positioned 15 mm from the columns, and the light intensity was measured using a Radiometer (VLX-3W Radiometer 9811-50, Cole Palmer) at 254 nm (UV-C region). The intensity of a single UV lamp measured by the Radiometer at the distance of 15 mm from the lamp was 4.1 mW cm^{-2}. The external surface of the reactor was covered with aluminum foil for UV-safety.

Reactions were performed under atmospheric pressure at room temperature. The reaction solutions were prepared by dilution of the stock solutions, and the aqueous phase was then introduced into the reservoir. The initial pH of the reaction solution was adjusted to pH 7.0 (± 0.4), except in the pH experiment. The reaction solution was transferred to the sample collector and reservoir using a three-way valve. The top of the reservoir bottle remained open to expose the solution to atmospheric pressure.

Sample Analysis

Samples of 10 ml each were taken from the reaction mixture at regular intervals and filtered through MCE membrane filters with a 0.2-μm pore size (Advantec MFS Inc.) to remove TiO_2 particles prior to analysis. The filtrate was then used to determine the RDX and HMX concentrations. The RDX and HMX concentrations were measured by HPLC using a Summit™ HPLC system (Dionex) equipped with a UVD 340S photodiode array detector (Dionex) set at 254 nm, and EPA method 8330 was used [20,21]. An isocratic eluent mixture of methanol and water (50:50, v/v) was used at a flow rate of 1.0 ml min^{-1}. A C-18 Supelco silica column (25 cm, 4.6 mm i.d., 5 μm particles) and a guard column (All-guard Adsorbosphere C18-5V; Phenomenex Inc.) were used and replaced regularly.

The analysis of total organic carbon (TOC) was performed on a Shimadzu TOC analyzer (Shimadzu). Among the ionic byproducts of the degradation, formate, NO_2^-, and NO_3^- were measured with a DX-120 ion chromatograph (Dionex). A Dionex Ion Pac AS14 column was used to measure NO_2^- and NO_3^- with a mixture of 3.5 mM Na_2CO_3 and 1 mM $NaHCO_3$ as an eluent. For the analysis of formate, an Ion Pac AS4A-SC column was used with 5.0 mM $Na_2B_4O_7$. The NH_4^+ ion was measured with an ion chromatograph using an Ion Pac CS12-A column (Dionex) with 20 mM of methyl sulfonate as an eluent.

RESULTS AND DISCUSSION

Comparison of RDX Degradation with and without Photocatalysis

To confirm the role of TiO_2 in the photocatalysis reaction, three sets of experiments were performed to compare RDX degradation rates with and without catalysts. One set was performed with RDX (20 mg l^{-1}) exposed to TiO_2 (1 g l^{-1}) but not UV (TiO_2-only condition). The second set was performed by exposing RDX (30 mg l^{-1}) to UV without TiO_2 (photolysis condition). The third set was performed by exposing RDX to TiO_2 (1 g l^{-1}) in the presence of UV illumination (photocatalysis condition). The results are presented in Figure 3.

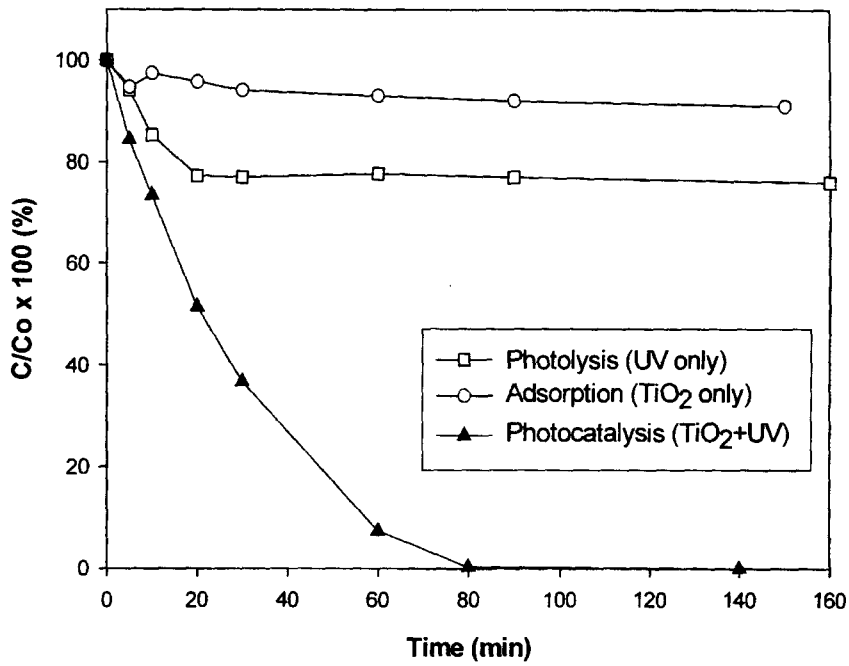

Figure 3. RDX degradation under control conditions (TiO_2-only and UV-only) and photocatalytic conditions.

The TiO_2-only experiments showed that only a trace amount of RDX (about 5%) was removed, and adsorption to TiO_2 is the most probable mechanism, with similar results being observed before in our laboratory with other compounds [22] and by others [23]. The RDX concentration stabilized after 20 minutes and not more than 5% of the initial RDX was adsorbed. Figure 4 is dramatic evidence demonstrating that UV light is required for degradation. In this experiment, RDX and HMX were combined with TiO_2. No degradation occurred in the first 60 minutes (no UV exposure) and rapid degradation was observed after illumination with UV light. The NO_2^- and NO_3^- byproducts confirm degradation and are described later. The photolysis reaction resulted in approximately 20% decrease in the RDX concentration after 80 min, whereas RDX (30 mg l^{-1}) was completely removed after 80 min under the photocatalysis condition (Figure 3). Several studies have shown that photolysis and photocatalysis share the same degradation pathway and that the difference in the reaction rates between the two processes is attributable to the hydroxyl radical concentration [24,25].

Mineralization and Organic Intermediates from RDX/HMX Photocatalysis

Given the unavailability of labeled RDX and HMX compounds, TOC measurements were performed instead to provide indirect evidence of mineralization during RDX and HMX photocatalysis. The results of RDX and HMX degradation and TOC measurements are shown in Figure 5. The degradation of HMX was relatively quick; no HMX was detected by HPLC after 30 min, while RDX was still detected after 60 min. Figure 5 also shows that approximately 60% of the TOC was removed within 150 min of HMX photocatalysis, but only 20% of the TOC was mineralized by RDX photocatalysis. The low conversion of TOC in the RDX photocatalysis is believed to occur because of the presence of organic byproducts from the photocatalysis of RDX. The TOC result with HMX photocatalysis indicates that the majority of the degraded HMX is converted to CO_2 or is mineralized. Such differences between degradation rates and TOC removal rates resulted from the different initial concentrations required by their different solubilities.

To confirm the mineralization during photocatalysis, the organic intermediates of RDX and HMX photocatalysis were measured using an ion chromatograph. In the experiments, two UV lamps (4.1 × 2 mW cm^{-2}) were used instead of four in order to decrease the degradation rates, to enable more precise measurements of the short-lived intermediates. Figure 6(a) shows that a trace amount of formate (accounting for a maximum of 2% of the carbon in RDX) was produced from RDX photocatalysis, while more formate (maximum 6%) was produced by HMX photocatalysis (Figure 6(b)). The observation of more formate during HMX photocatalysis may be due to the greater degradation of HMX. The produced formate was found to be rapidly mineralized to CO_2 by TiO_2 photocatalysis [11].

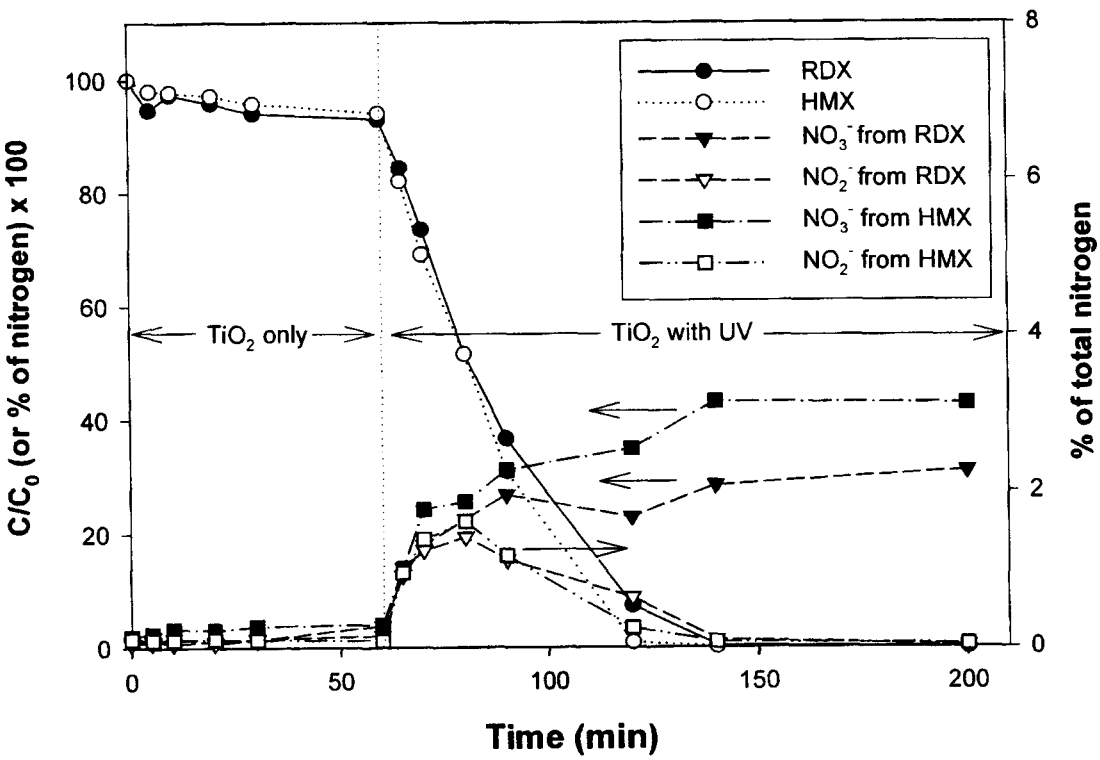

Figure 4. Percent of total nitrogen produced during adsorption and photocatalysis of RDX and HMX ($[RDX]_o$ = 20 mg l^{-1}, $[HMX]_o$ = 5 mg l^{-1}).

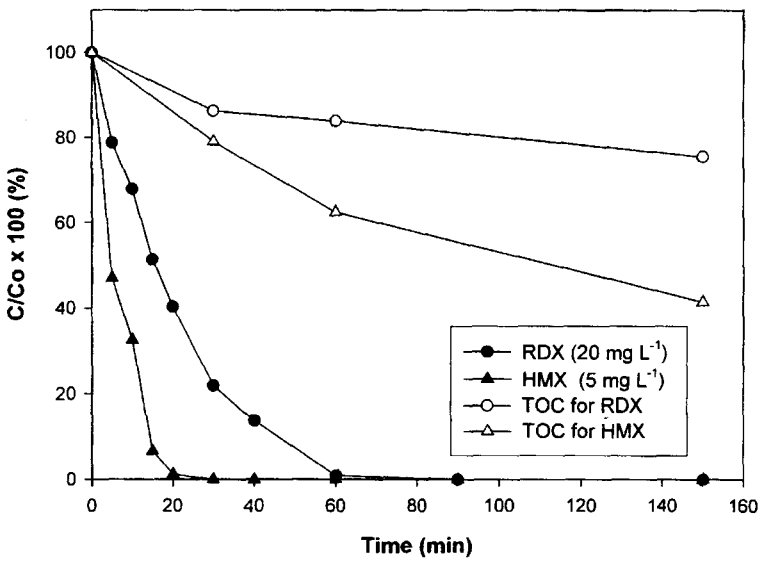

Figure 5. A comparison of the removal efficiency and TOC degradation of RDX and HMX under photocatalysis and photolysis.

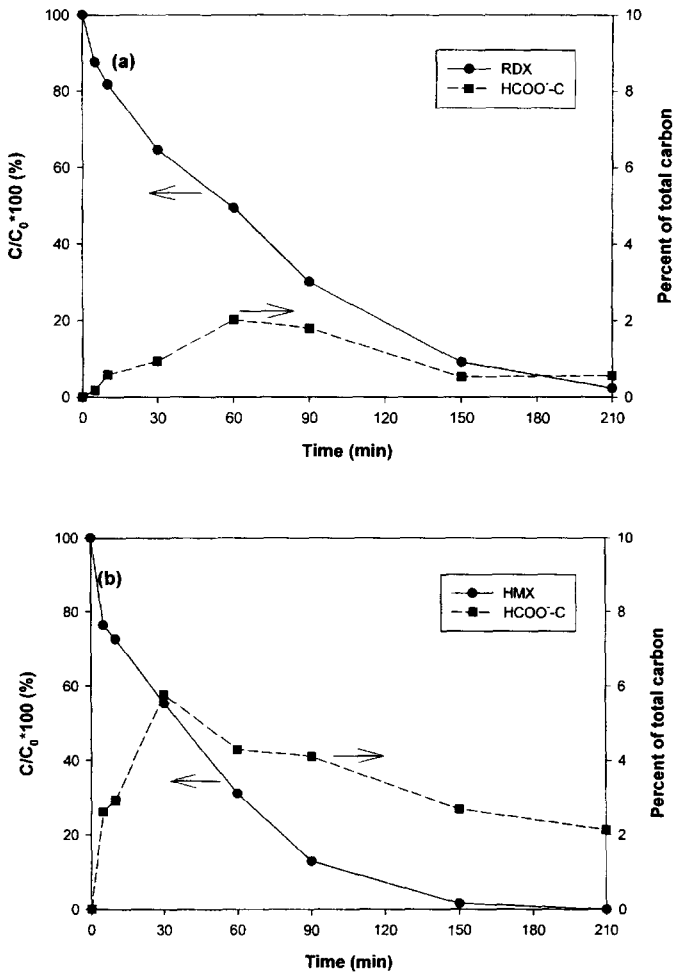

Figure 6. Change in concentration of formate during the photocatalytic degradation of (a) RDX and (b) HMX ($[RDX]_o$ = 20 mg l^{-1}, $[HMX]_o$ = 5 mg l^{-1}).

Formation of Nitrogen Byproducts

The formation of nitrogen byproducts from photocatalysis is expected, as both RDX and HMX contain several nitro groups (NO_2) that are susceptible to oxidation or reduction in photocatalytic reactions. The nitrogen byproducts created during RDX and HMX photocatalysis were measured using ion chromatography and are shown in Figure 7(a), and the corresponding results for the photocatalysis of HMX are shown in Figure 7(b). The concentrations of RDX and HMX and the nitrogen byproducts are represented as the percentage of nitrogen.

Figure 7(a) shows that NO_2^-, NO_3^-, and NH_4^+ ions were produced as the nitrogen byproducts in the photocatalytic reaction of RDX. Figure 7(a) also shows that the concentration of NO_2^- increased initially and then decreased and that the maximum concentration of NO_3^- was reached when the NO_2^- concentration decreased to zero. This pattern indicates that NO_2^- was separated from the RDX molecules during the photocatalytic reaction and that it became rapidly oxidized to

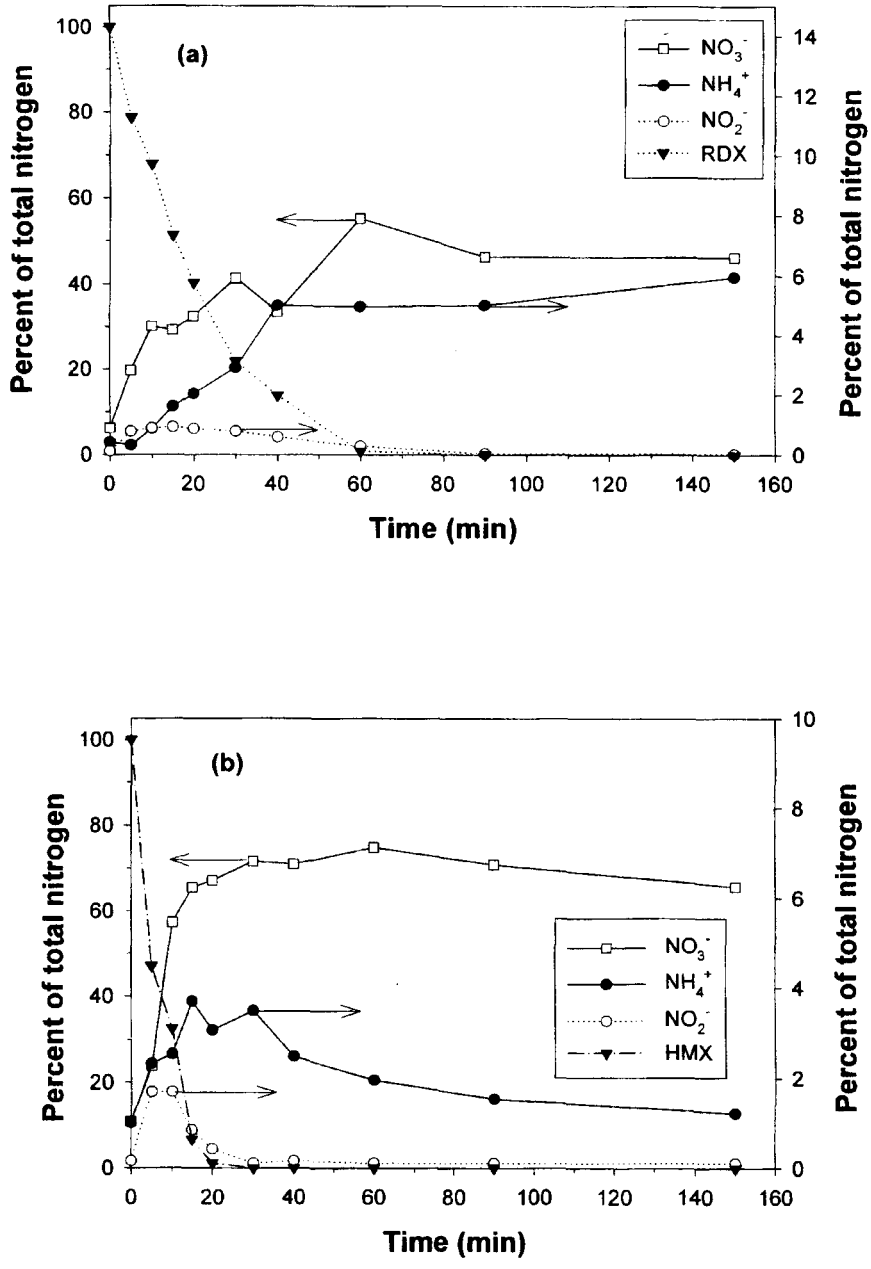

Figure 7. Formation of NO_3^-, NO_2^-, and NH_4^+ ions during the photocatalytic degradation of (a) RDX and (b) HMX ($[RDX]_o$ = 20 mg l^{-1}, $[HMX]_o$ = 5 mg l^{-1}).

NO_3^- by hydroxyl radicals. At the end of the reaction, about 50% of the nitrogen initially present in the RDX had been converted to NO_3^-, and about 6% of the total nitrogen had been converted to NH_4^+.

The NO_3^- ion was the most predominant nitrogen byproduct, indicating that oxidation is the primary mode of the RDX photocatalysis. The conversion of NO_2^- to NO_3^- by hydroxyl radicals has been observed previously. The NO_2^-, NO_3^-, and NH_4^+ ions are known to form as the transformation products of nitro-aromatic and ring compounds in AOP processes [14, 26]. The amount of nitrogen converted to NO_2^-, NO_3^-, and NH_4^+ after 160 min of the RDX photocatalysis reaction accounted for approximately 60% of the total initial nitrogen. The lack of nitrogen mass balance on complete degradation of RDX might result from the formation of two classes of compounds, nitrogen-containing organic intermediates and molecular nitrogen, resulting in a loss of nitrogen from the system.

The formation of NH_4^+ ions during RDX photocatalysis indicates a concurrent reduction reaction during the photocatalysis of RDX. The reduction of nitro groups to amines by electrons (e^-_{CB}), produced along with holes (h^+_{VB}) by illuminating TiO_2 with UV, has been proposed by Piccinini et al. [27]. The resulting amine groups can be detached from the main compound via the ring opening and the carbon-carbon breakage can be done by hydroxyl radicals.

A similar pattern in the production of nitrogen byproducts was observed in the HMX photocatalysis. Figure 7(b) shows that NO_2^-, NO_3^-, and NH_4^+ ions were produced in the HMX photocatalysis. More nitrogen was recovered in the HMX photocatalysis than in the RDX photocatalysis; slightly more than 70% of the total nitrogen in HMX was converted mainly to NO_3^- via NO_2^-, and NH_4^+.

Effect of initial RDX Concentration

The effect of initial RDX concentration on the photocatalytic degradation rate was investigated. The Langmuir-Hinshelwood kinetic expression has been used in heterogeneous photocatalysis to describe the relationship between initial degradation rates and initial concentrations [28-31]. In this model, the reaction rate for the second-order surface decomposition of explosives is written as follows:

$$\text{rate} = -\frac{d[HE]}{dt} = k_c \frac{K_{HE}[HE]}{1 + K_{HE}[HE]_o} \quad \text{(i)}$$

where $[HE]$ is the concentration of highly explosive compounds (RDX or HMX) at time t, k_c is the second-order rate constant, K_{HE} is the equilibrium adsorption constant of explosive compounds onto TiO_2, and $[HE]_o$ is the initial concentration of high explosive compounds such as RDX and HMX. According to Eq. (i), the photocatalytic degradation of RDX or HMX in the presence of TiO_2 exhibits pseudo-first-order kinetics with respect to the concentration of the explosive, as follows:

$$-\frac{d[HE]}{dt} = k_{obs}[HE] = k_c \frac{K_{HE}}{1 + K_{HE}[HE]_o}[HE] \quad \text{(ii)}$$

where k_{obs} is the observed pseudo-first-order rate constant for the photocatalytic oxidation of RDX or HMX. The integration of Eq. (ii) results in:

$$\ln\left(\frac{[HE]}{[HE]_o}\right) = -k_{obs}t \quad \text{(iii)}$$

Based on this model, the RDX degradation rate of TiO_2 photocatalysis over the concentration range of 1 to 50 mg l^{-1} RDX was investigated (see Figure 8). The experiment using different initial HMX concentrations was not performed because the concentration ranges of HMX are constrained by its solubility limit.

Figure 8(a) shows that the degradation rate decreased as the initial RDX concentration increased, indicating that the RDX degradation kinetics are not simple first-order but are pseudo-first-order, based on the Langmuir-Hinshelwood model. Based on Eq. (ii), a straight-line relationship of $ln([HE]_o/[HE])$ versus irradiation time during RDX photocatalysis was observed, as indicated in Figure 8(b) and Table 1.

The relationship between k_{obs} and $[HE]_o$ from Eq. (ii) can be expressed as follows:

$$\frac{1}{k_{obs}} = \frac{1}{k_c K_{HE}} + \frac{[HE]_o}{k_c} \quad \text{(iv)}$$

Eq. (iv) shows that a linear expression can also be obtained by plotting the reciprocal of the degradation rate ($1/k_{obs}$) as a function of the initial RDX concentration. Based on this equation, the values of k_{obs} at different initial RDX concentrations were fitted and plotted in Figure 9. The adsorption equilibrium constant (K_{HE}) and the second order rate constant (k_c) for RDX photocatalysis were obtained, 8.88 l mg^{-1} and 1.70 mg l^{-1} min^{-1}, respectively, using a least squares fit.

Effect of TiO_2 Catalyst Loading

To determine the effect of the amount of TiO_2 on the degradation of the explosives, varying quantities of TiO_2, ranging from 0 to 1.5 g l^{-1}, were added to a solution of 1.0 mg l^{-1} HMX, which was then irradiated with 15-W UV lamps for 90 min. To minimize the direct photolysis effects of the light source, only two UV lamps (4.1 × 2 mW cm^{-2}) were used. Samples taken during the reaction were analyzed, and the results are shown in Figure 10. When the HMX solution was

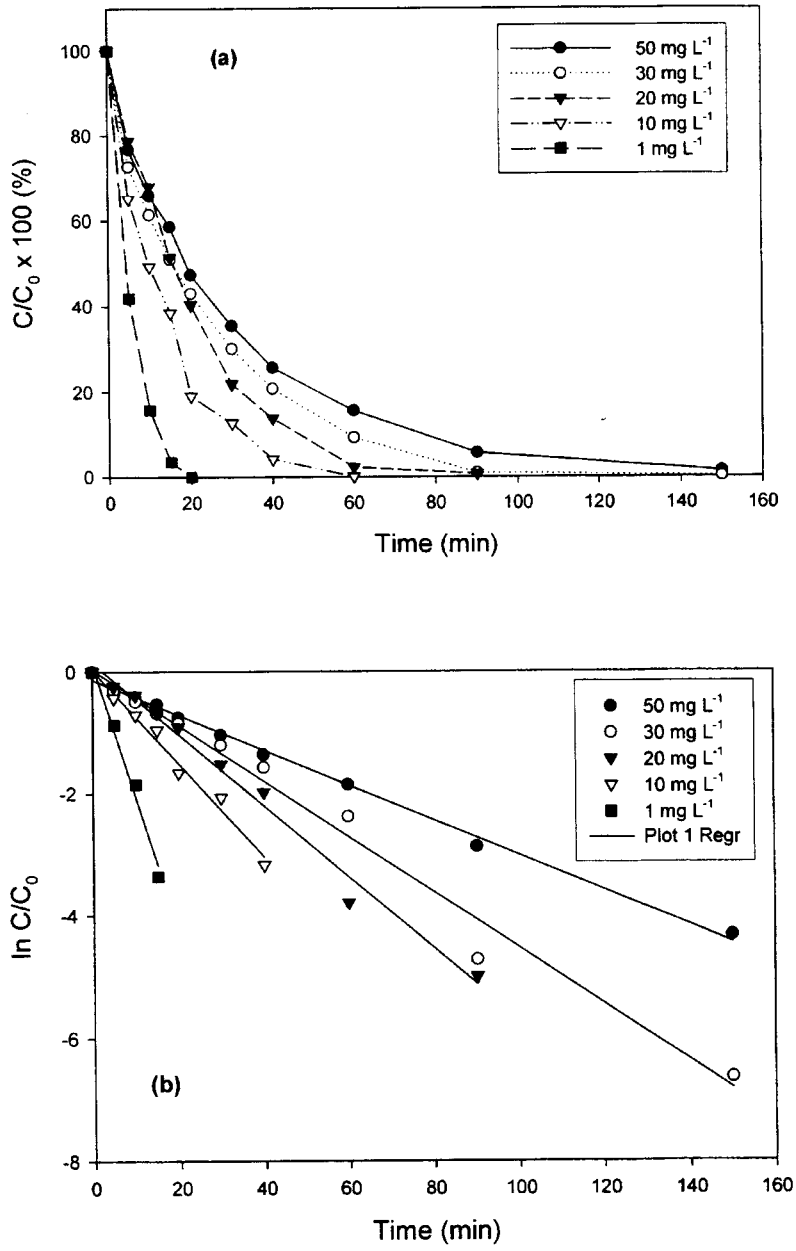

Figure 8. Effect of initial RDX concentration on the removal efficiency: (a) the percent removal of RDX at different initial RDX concentrations, and (b) $ln(c_o/c)$ versus irradiation time.

Table 1. The observed first-order rate constants k_{obs}, half-lives $t_{1/2}$, and correlation coefficients R^2 for the degradation of different initial concentrations of RDX

Initial RDX concentration (mg l^{-1})	k_{obs} (min^{-1})	$t_{1/2}$ (min)	R^2
1	0.2091	3.31	0.978
10	0.0756	9.17	0.983
20	0.0559	12.4	0.984
30	0.0453	15.3	0.994
50	0.0303	22.9	0.990

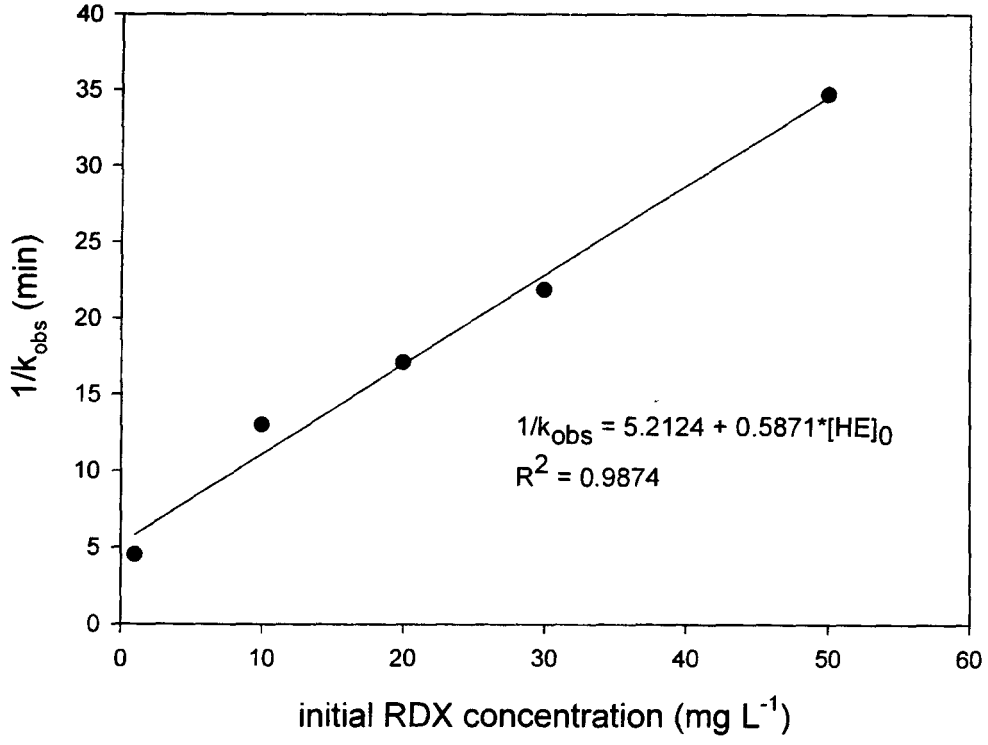

Figure 9. The initial RDX concentration versus the reciprocal of the observed first-order rate constant ($1/k_{obs}$).

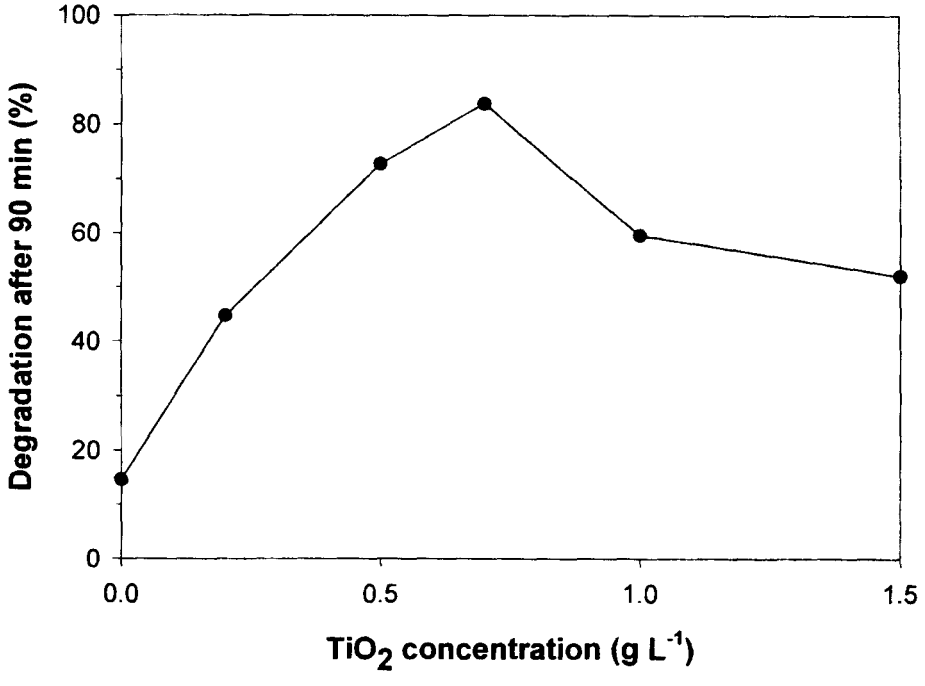

Figure 10. Effect of TiO_2 dosage on the photocatalytic degradation of HMX ($[HMX]_o$ = 1 mg l^{-1}, UV_{254nm} = 4.1 × 2 mW cm^{-2}).

irradiated without TiO_2, the removal of HMX was only 15% and was due to direct photolysis. The percentage of HMX degraded at 90 min increased with higher TiO_2 concentrations, up to concentrations of 0.7 g l^{-1}. At TiO_2 concentrations higher than 0.7 g l^{-1}, the degradation efficiency of HMX decreased. At high concentrations, TiO_2 particles can block UV light from reaching the TiO_2 surface, or light scattering by the TiO_2 particles may decrease the HMX degradation efficiency [32].

Effect of pH

As pH can influence the surface charge of TiO_2 and shift the potential of some redox reactions, it can be a strong factor controlling the adsorption of contaminants and the reactivity of TiO_2, and thus the reaction rate. Therefore, we investigated the impact of the initial pH on the degradation of RDX and HMX.

First, the initial RDX (20 mg l^{-1}) and HMX (5 mg l^{-1}) solutions were adjusted to the appropriate pH (pH = 3, 7, or 11) with 1 N NaOH or 1 N HCl. The solutions were irradiated with two UV lamps and treated with 1.0 g l^{-1} of TiO_2. Then, the rate constants of RDX and HMX degradation were measured at each pH. The results (see Table 2) show that RDX and HMX degradation was least effective at acidic pH values and was higher at neutral and basic pH levels.

When titanium dioxide (TiO_2) is illuminated with light of band gap energy, electrons in conduction bond (e^-_{CB}) and holes in valence bond (h^+_{VB}) are produced according to Eq. (v):

$$TiO_2 + h\nu \rightarrow h^+_{VB} + e_{CB}^- \quad \text{(v)}$$

These charge carriers can recombine, or the holes can be scavenged by oxidizing species (for example, H_2O, OH^-), and electron by reducible species (for example, O_2) in the solution [33]:

$$h^+_{VB} + H_2O \rightarrow \cdot OH + H^+ \quad \text{(vi)}$$

$$h^+_{VB} + OH^- \rightarrow \cdot OH \quad \text{(vii)}$$

$$e^-_{CB} + O_2 \rightarrow \cdot O_2^- \quad \text{(viii)}$$

The hydroxyl radical ($\cdot OH$) is likely the dominant oxidizing species in the photocatalytic process, the photodegradation of RDX (or HMX) is therefore accelerated with increasing initial pH. The rate increment is likely due to the increase in hydroxyl ions (OH^-) in the solution. The quantity of OH^- ions on the surface of TiO_2 increased as the pH increases, and these ions can combine with holes (h^+_{VB}) to produce more OH radicals, as shown in Eq. (vii). Similar reactions have been suggested by a number of researchers [34-36].

The higher degradation rate at neutral pH also can be explained by the point of zero charge (p_{zc}) of TiO_2, which occurs at pH 6.25 [34, 37, 38]. The TiO_2 surface is positively charged in acidic media (pH < 6.25) and is negatively charged under alkaline conditions (pH > 6.25). As TiO_2 exhibits an amphoteric character with a zero charge in the pH range from about 6.2 to 6.4, the adsorption of RDX and HMX can be favorable at a pH near the p_{zc} of TiO_2. Therefore, higher RDX and HMX degradation efficiencies are to be expected at neutral pH. However, further increments of pH would retard the rates. This can be explained by the effect of charges of attraction or repulsion between TiO_2 particles and RDX (or HMX), or hydroxide ions (OH^-).

The pH experiment also showed that the pH of the solution decreased during the photocatalysis of RDX and HMX. This pH drop can be explained by two reactions: the decrease in hydroxide ion (OH^-) concentrations owing to the production of OH radicals, and the production of low-molecular-weight organic acids, such as formic acid, in the oxidation process during RDX/HMX degradation. Therefore, the TiO_2 is rapidly hydrated in aqueous solutions, according to the following equation [39]:

(ix)

Table 2. The observed first-order rate constants k_{obs}, half-lives $t_{1/2}$, and correlation coefficients R^2 for the degradation of RDX (20 mg l^{-1}), and HMX (5 mg l^{-1}) at different pH values

		k_{obs} (min^{-1})	$t_{1/2}$ (min)	R^2
RDX	pH 3	0.0367	18.9	0.996
	pH 7	0.0506	13.7	0.984
	pH 11	0.0460	14.4	0.999
HMX	pH 3	0.0773	8.97	0.978
	pH 7	0.2067	3.35	0.967
	pH 11	0.1127	6.15	0.990

where TiO_2 represents titanium dioxide in bulk solid phase and Ti(IV) is surface titanium. The hydrated TiO_2 surface is amphoteric and, accordingly, has a pH-dependent speciation. The equilibrium among the surface species can be described by:

$$[Ti(IV)]-OH_2^+ \xleftrightarrow{\pm H^+} [Ti(IV)]-OH \xleftrightarrow{\pm OH^-} [Ti(IV)]-O^- + H_2O \quad (x)$$

With regard to the economical and practical aspects of treatment, the results of the pH experiment imply that pH adjustment steps are not required in the treatment of RDX- or HMX-contaminated water with TiO_2 photocatalysis, provided the water has a neutral pH.

Proposed Mechanism

Based on these findings, we suggest a general pathway for the mineralization of RDX using TiO_2 photocatalysis. The suggested pathway is shown in Figure 11. In the

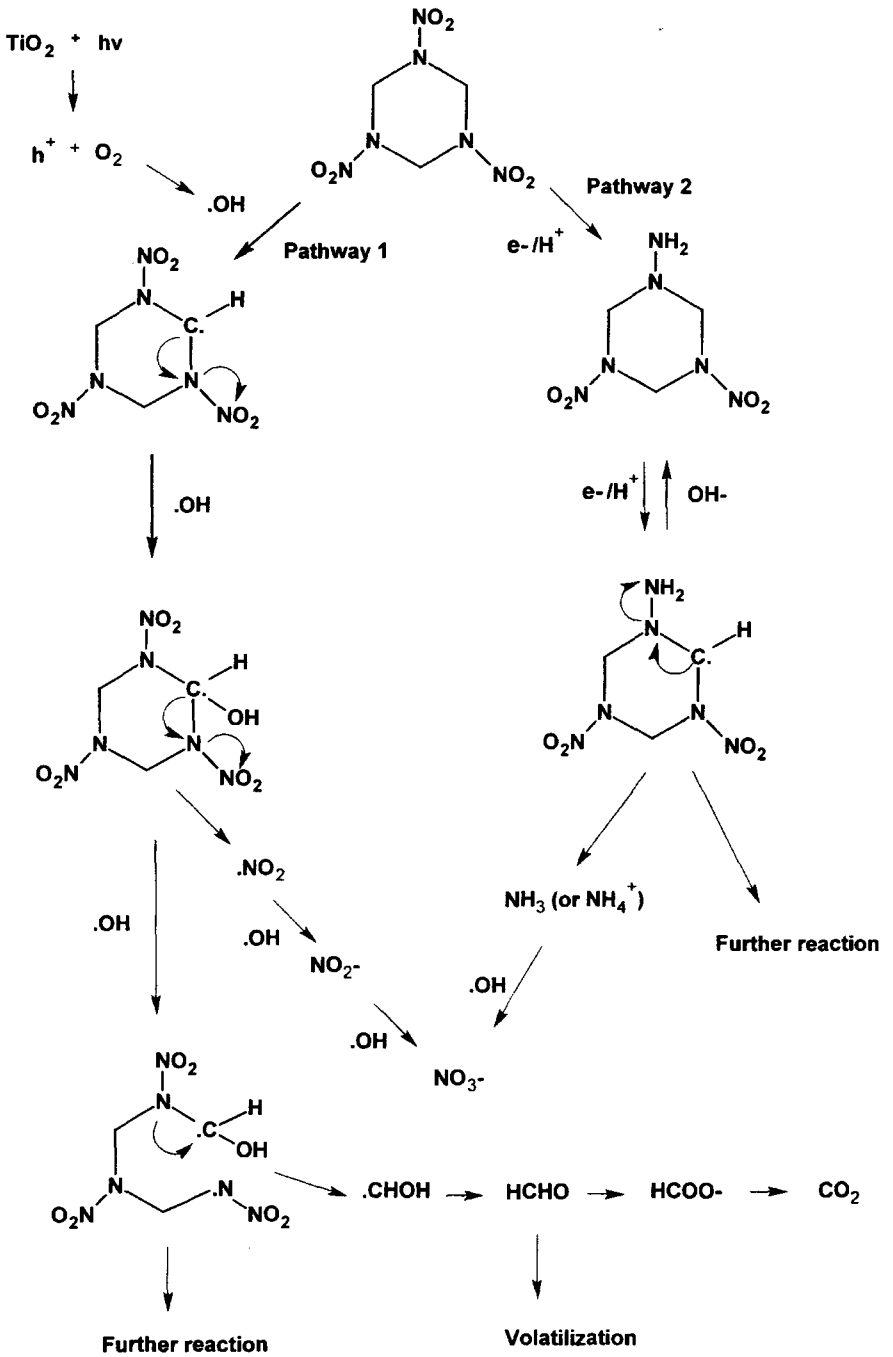

Figure 11. The proposed mechanism of RDX photocatalysis.

photocatalysis, the main oxidizing species is the hydroxyl radical (·OH). The first pathway in the RDX mineralization process can be initiated by the addition of hydroxyl radicals to the carbon of RDX (pathway 1). The resulting carbon radicals can undergo destruction of the N-NO_2 bonds to produce NO_2 radicals. These NO_2 radicals can further react with hydroxyl radical to release NO_3^-, which we observed by ion chromatography. Next, the resulting carbon radicals can undergo ring breakage to form ·CHOH radicals. These radicals can be further transformed to formaldehyde which can be volatilized into the atmosphere or further transformed to formate, a compound identified from the experiments. The formate produced by RDX degradation is known to be mineralized to CO_2 [11].

The formation of NH_4^+ during the photocatalysis of RDX is proposed in pathway 2. The reduction of the nitro groups of RDX to amines by electrons (e_{CB}^-) is a direct hydroxylation, as proposed by Piccinini et al. [27]. The resulting amine groups can be detached from the main RDX compound and can exist as NH_3 or NH_4^+, depending on the pH. This species can be further oxidized to NO_3^- by hydroxyl radicals, as observed by Low et al. [26]. Based on molecular similarity, the degradation pathway for the mineralization of HMX using TiO_2 photocatalysis is likely to be similar to the RDX mechanism.

CONCLUSIONS

TiO_2 photocatalysis was evaluated for treating RDX- and HMX-contaminated water. Photocatalysis was successful in mineralizing both compounds. The conclusions are summarized as follows:

1. Degradation does not occur without UV irradiation, and only trace amounts of RDX and HMX (about 5% each) can be adsorbed to TiO_2.
2. Photolysis is much less effective than photocatalysis. Experiments using photolysis resulted in only 20% decrease in the RDX (20 mg l^{-1}) concentration after 90 min, whereas RDX was completely removed by photocatalysis during the same period.
3. RDX and HMX degradation followed a pseudo-first-order rate expression, according to the Langmuir-Hinshelwood kinetic model.
4. The degradation rate of HMX increased as the amount of TiO_2 increased until the concentration of TiO_2 exceeded 0.7 g l^{-1}, at which point the reaction rate decreased. The decreased reaction was probably due to interference of the high concentration of TiO_2 particles with UV light absorption.
5. RDX and HMX showed higher photocatalytic degradation efficiencies at neutral pH than at pH 3 or 11, and the solution pH decreased during the reaction owing to the hydration of TiO_2 and formation of simple organic acids (e.g., formic acid).
6. NO_3^- was a major byproduct of both RDX and HMX photocatalysis. The produced NO_2^- was rapidly oxidized to NO_3^- by the hydroxyl radical. Trace amounts of NH_4^+ were also observed.
7. Formate was qualitatively identified as an organic intermediate in RDX and HMX degradation and was further mineralized. The TOC data indicated that other unidentified organic intermediates were also formed.
8. Two mechanistic pathways of RDX photocatalysis were proposed, one via the reaction between RDX and OH radicals, and the other via the reaction between RDX and electrons.

The results of this study indicate that the TiO_2 photocatalytic system could be used as a treatment alternative for *ex-situ* remediation of explosives-contaminated groundwater.

ACKNOWLEDGEMENTS

This work was supported by the Seoul National University Foundation & Overhead Research Fund.

REFERENCES

1. Spalding R.F. and Fulton J.W., Groundwater munitions residues and nitrate near Grand Island, Nebraska, U.S.A.. *J. Contam. Hydrol.*, **2**, 139-146 (1998).
2. Yinon J., *Toxicity and Metabolism of Explosives*. CRC Press, Boca Raton, FL, USA. pp. 81-122 (1990).
3. Burton D.T., Turley S.D. and Peters G.T., The acute and chronic toxicity of hexahydro-1,3,5-trinitro-1,3,5-triazine (RDX) to the fathead minnow (*Pimephales promelas*). *Chemosphere*, **29**, 567-579 (1994).
4. Burton D.T., Turley S.D. and Peters G.T., The toxicity of hexahydro-1,3,5-trinitro-1,3,5-triazine (RDX) to the freshwater green alga *Selenastrum-capricornutum*. *Water, Air Soil Pollut.*, **76**, 449-455 (1994).
5. Peters G.T., Burton D.T., Paulson R.L. and Turley S.D., The acute and chronic toxicity of hexahydro-1,3,5-trinitro-1,3,5-triazine (RDX) to 3 freshwater invertebrates. *Environ. Toxicol. Chem.*, **10**, 1073-1081 (1991).
6. Kaplan D.L., Biological degradation of explosives and chemical agents. *Curr. Opin. Biotechnol.*, **3**, 253-260 (1992).
7. McLellan W., Hartley W.R., Brower M., Health Advisory for Octahydro-1,3,5,7-Tetranitro-1,3,5,7-Tetrazocine; Technical

Report No. PB90-273533, Office of Drinking Water, U.S. Environmental Protection Agency, Washington, D.C. (1998).
8. Alnaizy R. and Akgerman A., Oxidative treatment of high explosives contaminated wastewater. *Water Res.*, **33**, 2021-2030 (1999).
9. Etnier E.L. and Hartley W.R., Comparison of water quality criterion and lifetime health advisory for hexahydro-1,3,5-trinitro-1,3,5-triazine (RDX). *Regulatory Toxicol. Pharmacol.*, **11**, 118-125 (1990).
10. McLellan W.L., Hartley W.R. and Brower M.E., Hexahydro-1,3,5-trinitro-1,3,5-triazine (RDX), *Drinking Water Health Advisory: Munitions*, Robert W.C. and Hartley W.R. (Ed.), Lewis Publishers, Boca Raton, FL, USA. pp. 130-180 (1992).
11. Carraway E.R., Hoffman A.J. and Hoffman M.R., Photocatalytic oxidation of organic acids on quantum-sized semiconductor colloids. *Environ. Sci. Technol.*, **28**, 786-793 (1994).
12. Maugans C.B. and Akgerman A., Catalytic wet oxidation of phenol over a Pt/TiO_2 catalyst, *Water Res.*, **31**, 3116-3124 (1997).
13. Bose P., Glaze W.H. and Maddox D.S., Degradation of RDX by various advanced oxidation processes: I. reaction rates. *Water Res.*, **32**, 997-1004 (1998).
14. Bose P., Glaze W.H. and Maddox D.S., Degradation of RDX by various advanced oxidation processes: II. organic by-products. *Water Res.*, **32**, 1005-1018 (1998).
15. Zoh K.D. and Stenstrom M.K., Fenton oxidation of hexahydro-1,3,5-trinitro-1,3,5-triazine (RDX) and octahydro-1,3,5,7-tetranitro-1,3,5,7-tetrazocine (HMX). *Water Res.*, **36**, 1331-1341 (2002).
16. Lee S.J., Son H.S., Lee H.K. and Zoh K.D., Photocatalytic degradation of explosives contaminated water. *Water Sci. Technol.*, **46**, 139-145 (2002).
17. Topalov A., Molnar-Gabor D. and Csanadi J., Photocatalytic oxidation of the fungicide metalaxyl dissolved in water over TiO_2, *Water Res.*, **33**, 1371-1376 (1999)
18. Herrera Melian J.A., Dona Rodrõguez J.M., Viera Suarez A., Tello Rendon E., C. Valdes do Campo C., Arana J. and Perez Pena J., The photocatalytic disinfection of urban waste waters. *Chemosphere*, **41**, 323-327 (2000).
19. Rosenblatt D.H., Burrows E.P., Mitchell W.R. and Parmer D.L., Organic explosives and related compounds. In: *The Handbook of Environmental Chemistry*, vol. 3, Part G, Hutzinggen O. (ed.), Springer, Berlin, Germany, pp. 195–232 (1991).
20. US EPA, Nitroaromatics and nitramines by high perfromance liquid chromatography (HPLC). SW-846, Method 8330. Revision 4, US Environmental Protection Agency, Washington. D.C. (1994).
21. US EPA, EPA Method 8330, SW-846 update III, Part 4(B). Office of Solid Waste, US Environmental Protection Agency Washington D.C. (1997).
22. Son H.S., Lee S.J., Cho I.H. and Zoh K.D., Kinetics and mechanism of TNT degradation in TiO_2 photocatalysis. *Chemosphere*, **57**, 309-317 (2004).
23. Bekkouche S., Bouhelassa M., Hadj Salah N., and Meghlaoui F.Z., Study of adsorption of phenol on titanium oxide (TiO_2). *Desalination*, **166**, 355-362 (2004).
24. Schmelling D.C. and Gray K.A., Photocatalytic transformation and mineralization of 2,4,6-trinitrotoluene (TNT) in TiO_2 slurries. *Water Res.*, **29**, 2651-2662 (1995).
25. Goutailler G., Valette J.C., Guillard C., Paisse O. and Faure R., Photocatalysed degradation of cyromazine in aqueous titanium dioxide suspensions: comparison with photolysis. *J. Photochem. Photobiol. A: Chem.*, **141**, 79-84 (2001).
26. Low G., McEvoy S.R., Stephan M.A. and Matthews R.W., Formation of nitrate and ammonium ions in titanium dioxide mediated photocatalytic degradation of organic compounds containing nitrogen atoms. *Environ. Sci. Technol.*, **25**, 460-467 (1991).
27. Piccinini P., Minero C., Vincenti M. and Pelizzetti E., Photocatalytic interconversion of nitrogen-containing benzene derivatives. *J. Chem. Soc. Faraday Trans.*, **93**, 1993-2000 (1997).
28. Al-Sayyed G., D'Oliveira J.C., and Pichat P., Semiconductor-sensitized photo-degradation of 4-chlorophenol in water. *J. Photochem. Photobiol. A Chem.*, **58**, 99-114 (1991).
29. Lu M.C., Roam G.D., Chen J.N. and Huang C.P., Factors affecting the photocatalytic degradation of dichlorovos over titanium dioxide supported on glass. *J. Photochem. Photobiol. A Chem.*, **76**, 103-110 (1993).
30. Mills G. and Hoffmann M.R., Photocatalytic degradation of pentachlorophenol on TiO_2 particles-identification of intermediates and mechanisms of reaction. *Environ. Sci. Technol.*, **27**, 1681-1689 (1993).
31. Chen D. and Ray A.K., Photodegradation kinetics of 4-nitrophenol in TiO_2 suspension. *Water Res.*, **32**, 3223-3234 (1998).
32. Prairie M.R., Evans N.R., Stange B.M. and Martinez S.L., An investigation of TiO_2 photocatalysis for the treatment of water contaminated with metals and organic chemicals. *Environ. Sci. Technol.* **27**, 1176-1782 (1993).
33. Okamoto K., Yamamoto Y., Tanaka H., Hanaka M. and Itaya A., Heterogeneous photocatalytic decomposition of phenol over TiO_2 powder. *Bull. Chem. Soc. Jpn.* **58**, 2015-2022 (1985).
34. Ollis D.F., Pelizzetti E. and Serpone N., Destruction of water contaminants. *Environ. Sci. Technol.* **25**, 1523–1529 (1991).
35. Bianco-Prevot A., Vincenti M., Bianciotto A. and Pramauro E., Photocatalytic and photolytic transformation of chloramben in aqueous solutions. *Appl. Catal. B: Environ.* **22**, 149–158 (1999).

36. Sanchez L., Peral J. and Domenech X., Photocatalyzed destruction of aniline in UV-illuminated aqueous TiO_2 suspensions. *Electrochim Acta*, **42**, 1877–1882 (1997).
37. Poulios I. and Tsachpinis J., Photodegradation of the textile dye Reactive Black 5 in the presence of semiconducting oxides. *J. Chem. Technol. Biotechnol.*, **71**, 349-357 (1999).
38. Yang H.G., Li C.Z., Gu H.C. and Fang T.N., Rheological behavior of titanium dioxide suspensions. *J. Colloid. Interf. Sci.*, **236**, 96–103 (2001).
39. Peterson M.W., Turner J.A. and Nozik A.J., Mechanistic studies of the photocatalytic behavior of TiO_2: particles in a photochemical slurry cell and the relevance to photodetoxification reactions. *J. Phys. Chem.*, **95**, 221-227 (1991).